Stochastic Jetting and Dripping in Confined Soft Granular Flows

Michał Bogdan⬤,[1,*] Andrea Montessori⬤,[2] Adriano Tiribocchi,[3] Fabio Bonaccorso⬤,[3,4] Marco Lauricella,[3] Leon Jurkiewicz,[1] Sauro Succi,[3,5,6] and Jan Guzowski[1,†]

[1]*Institute of Physical Chemistry, Polish Academy of Sciences, Kasprzaka 44/52, 01-224 Warsaw, Poland*
[2]*Dipartimento di Ingegneria, Universit degli Studi Roma tre, via Vito Volterra 62, Rome 00146, Italy*
[3]*Istituto per le Applicazioni del Calcolo del Consiglio Nazionale delle Ricerche, via dei Taurini 19, 00185 Rome, Italy*
[4]*Department of Physics and National Institute for Nuclear Physics, University of Rome "Tor Vergata",*
Via Cracovia, 50, 00133 Rome, Italy
[5]*Center for Life Nanoscience at la Sapienza, Istituto Italiano di Tecnologia, viale Regina Elena 295, 00161 Rome, Italy*
[6]*Department of Physics, Harvard University, 17 Oxford Street, Cambridge, Massachusetts 02138, USA*

We report new dynamical modes in confined soft granular flows, such as stochastic jetting and dripping, with no counterpart in continuum viscous fluids. The new modes emerge as a result of the propagation of the chaotic behavior of individual grains—here, monodisperse emulsion droplets—to the level of the entire system as the emulsion is focused into a narrow orifice by an external viscous flow. We observe avalanching dynamics and the formation of remarkably stable jets—single-file granular chains—which occasionally break, resulting in a non-Gaussian distribution of cluster sizes. We find that the sequences of droplet rearrangements that lead to the formation of such chains resemble unfolding of cancer cell clusters in narrow capillaries, overall demonstrating that microfluidic emulsion systems could serve to model various aspects of soft granular flows, including also tissue dynamics at the mesoscale.

Soft granular materials consist of close-packed deformable grains separated by thin fluid films. They are ubiquitous in industries, forming food and cosmetic products and in nature, where examples include dense emulsions, foams, as well as certain types of biological tissues, among others [1–7]. The presence of the internal length scale in such materials, associated with the grain size, leads to a complex many-body dynamics governed by the sequences of grain deformations and rearrangements [8,9], which in turn result in complex flows and rheological behavior, including plasticity and viscoelasticity, memory effects, and avalanches [10–15].

The flow of such types of materials confined to narrow geometries is of primary interest to the physics of amorphous solids and glasses [8,9,16], as well as of technological relevance for the generation of compartmentalized capsules [17] and porous materials [18] or in bioprinting [19]. The dynamics of soft granular media in constrictions under external flow is also of significant interest in tissue mechanics [20], as it could shed light on the behavior of cell clusters passing through physiological constrictions, a process that remains one of the critical stages of tumor metastasis.

Previous microfluidic approaches to soft granular materials addressed the behavior of foams or dense emulsions inside channels, however, without considering the interaction with an external flow [8,9,13,21,22]. Here, we systematically study the behavior of a model soft-granular medium (a tightly packed monodisperse emulsion) under external viscous forces. We use a flow-focusing geometry in which the emulsion is fed through the middle channel and the external immiscible phase through the side channels. Accordingly, the emulsion is focused by the external flow and narrows until passing through an orifice, a situation which closely resembles the flow of cell clusters in capillaries.

Typically, in microfluidics, flow-focusing junctions are used to generate highly monodisperse emulsions [23]. Thus, in Newtonian liquids, one typically observes two primary dynamical modes: dripping, in which monodisperse droplets are created inside the orifice, and jetting, in which the focused phase flows in parallel with the focusing phase beyond the orifice, only to break-up much later [23–25] due to the Rayleigh-Plateau instability [24], although other regimes have also been reported [23,26,27].

Here, in the case of a granular medium, we find new dynamical patterns, distinct from simple viscous jetting and dripping, such as (i) formation of fluctuating jets in which the fluctuations of jet width are influenced by avalanche "discharge" of the dispersed granular phase at the junction rather than by the Rayleigh-Plateau instability of the jet,

(ii) formation of very thin jets—single-file chains of grains—via "unfolding" of thicker jets under extensional viscous stresses, and (iii) irregular breakup of the jets resulting in highly polydisperse grain clusters with a non-Gaussian size distribution. We highlight the stochasticity of the transport of the close-packed emulsion through the orifice in the various regimes and the impact of the behavior of individual grains on the dynamics of the entire emulsion (e.g., its breakup). Furthermore, we perform *ad hoc* numerical simulations based on a recently developed lattice Boltzmann method for multicomponent fluids with near-contact interactions [28–30] that reproduce the experimental findings. The simulations employ a perfectly monodisperse emulsion which demonstrates that the observed stochasticity of the system is intimately associated with the granular structure and not, in particular, with polydispersity of the droplets.

The droplets ("grains") of the innermost phase are reproducibly formed at a T junction of channels of rectangular cross sections. Subsequently, the monodisperse emulsion is pushed into a wider channel (see Fig. 1) and focused by the continuous phase into an orifice. We use three Newtonian liquids to formulate the double emulsion: fluorinated fluid [31] as the continuous phase, oil with surfactant as the middle (grain-lubricating) phase, and dyed water as the innermost grain phase (see Supplemental Material [32] for details). The T junction generates droplets at a volume fraction of 86% (the highest possible for which the emulsion is monodisperse and stable). Based on measured frequency of generation of the aqueous droplets, we estimate droplet volume to be around 11.4 nL which yields the diameter of an undeformed spherical droplet $D_0 = 0.28$ mm. Since the value of D_0 is larger than the channel height $H = 0.11$ mm, the droplets are flattened by the lower and upper walls. Based on the measured apparent areas of the generated clusters we estimate the diameter of the flattened droplets $D_\parallel = 0.37$ mm with a coefficient of variation $\mathrm{CV}_{D_\parallel} = 9.2\%$.
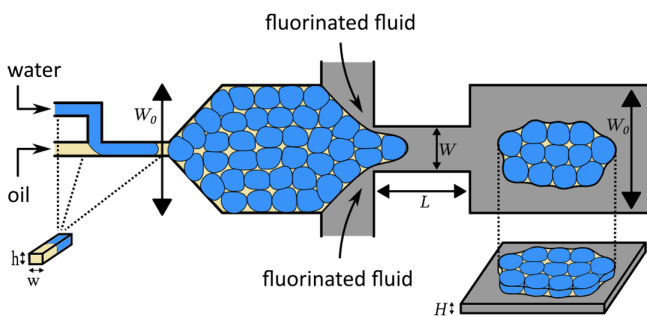

FIG. 1. Scheme of the microfluidic system for generation of a quasi-2D granular medium (water-in-oil emulsion) and its fragmentation under flow focusing with an external third immiscible phase (fluorinated fluid). Dimensions as measured by profilometry are $W_0 = 2$, $W = 1$, $L = 2$, $H = 0.11$, $w = 0.11$, and $h = 0.08$ mm.

The ensuing emulsion is stable enough to produce flows for several minutes, with only occasional coalescence of the aqueous droplets.

Our LB simulations, performed using a fully three-dimensional color-gradient approach augmented with near-contact interactions [28,29], use slightly different, but similar, parameters for the system and droplets. See Supplemental Material [32] and Ref. [33] for details on the simulation methods and implementation.

In the experiment, we change the flow rate of the continuous phase Q_c, while keeping the flow rate of the dispersed phase (the emulsion) Q_d constant and equal $Q_d = 0.5$ mL/h [34]. As a result, we observe several types of dynamic flow patterns as illustrated in Fig. 2, and movies SM1–SM4 in the Supplemental Material [32]. We find superficial similarity to jetting and dripping regimes present in simple fluids, however the observed dynamics is much richer. We can distinguish four different modes: (i) jetting with a large and moderately oscillating jet width, further referred to simply as *jetting*; (ii) jetting with thin, strongly oscillating jets and occasional breakup, further referred to as *oscillating jetting*; (iii) dripping resulting in a strongly polydisperse double emulsion, further referred to as *irregular dripping*; and (iv) dripping resulting in a relatively monodisperse double emulsion, further referred to simply as *dripping*. The numerical simulations recreate the same dynamical modes at values Q_c/Q_d similar to yet slightly
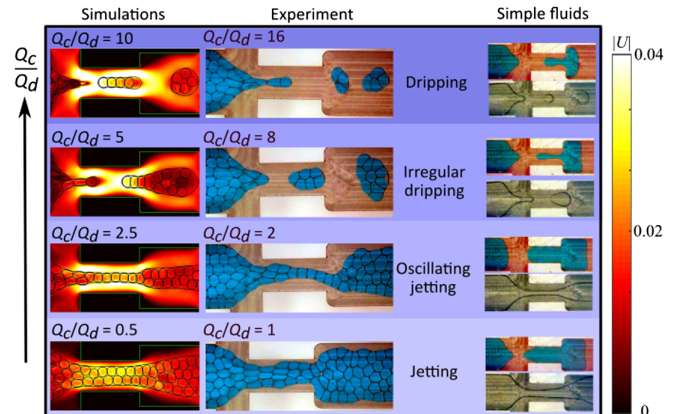

FIG. 2. Dynamical modes observed in the system upon varying Q_c/Q_d $Q_d = 0.5$ mL/h. Q_c/Q_d decreases from top to bottom (note different values for simulations and experiment). Smaller snapshots in the column on the right show flow patterns observed in the experiment with the emulsion replaced by a simple viscous liquid, either water (blue) or oil (transparent) for the same Q_c/Q_d as in the experiment with the emulsion. The color bar refers to simulation snapshots, with U being the local velocity in lattice units. Experimental snapshots were taken from movies SM1 ($Q_c/Q_d = 1$), SM2 ($Q_c/Q_d = 2$), SM3 ($Q_c/Q_d = 8$), SM 4 ($Q_c/Q_d = 16$); simulation-based snapshots are taken from movies SM5 ($Q_c/Q_d = 0.5$), SM6 ($Q_c/Q_d = 2.5$), SM7 ($Q_c/Q_d = 5$), and SM8 ($Q_c/Q_d = 10$) in the Supplemental Material [32].

different than the experimental ones, see Fig. 2 and movies SM5-SM8, in Ref. [32]. We attribute the differences to slightly different geometrical parameters and volume fractions as imposed by the numerical constrains (see Supplemental Material [32]).

In order to understand the impact of granularity of the focused fluid on the onset of oscillating jetting/irregular dripping regimes, we repeat the flow focusing experiment with a simple fluid (water or oil) as the dispersed phase. We find simple jetting (see SM9 and SM10 in Ref. [32] for oil at $Q_c/Q_d = 1$ and 2, respectively), highly monodisperse dripping ($CV_{A_\parallel} = 2.2\%$ for oil, where $A_\parallel$ is the area of a flattened oil drop, at $Q_c/Q_d = 3$; see SM11) or bidisperse dripping [35] (the latter, with 2 narrow peaks, in the case with oil at high Q_c/Q_d, see SM12 and SM13 for examples with $Q_c/Q_d = 4$ and 8, respectively; see Supplemental Material [32] for relevant histograms), but never observe irregular oscillations and rich dynamics similar to the case of a focused emulsion (see Fig. 2). In particular, we find only dripping for the case with water and the jetting-dripping transition for oil, which both agree with previous predictions for simple Newtonian liquids (i.e., that increasing viscosity of the dispersed phase promotes jetting) [26].

We further examine the four distinct dynamical modes observed for the focused emulsion in more detail. We define the minimum instantaneous jet width, $w_{\min}(t) = \min_{x\in[0,L]} w(x,t)$, where $w(x,t)$ is the full spatiotemporal profile of the jet within the narrowing, as a measure of jet oscillations in time [Fig. 3(a)]. We find that the corresponding time average, $\langle w_{\min}\rangle = T^{-1}\int_0^T dt\, w_{\min}(t)$, where T is the time of duration of the experiment, decreases upon increasing Q_c/Q_d while the stochastic fluctuations of $w_{\min}(t)$ remain of similar absolute magnitude. Accordingly, this leads to occasional break-up ($w_{\min} = 0$) of the jet in the oscillating jetting mode.

Additionally, in the jetting mode, we frequently observe abrupt granular "discharge" of the junction, associated with rapid entrance of several droplets in-parallel into the constriction. In order to quantify such avalanching behavior we measure the width of the jet $w_0(t)$ precisely at the entrance to the constriction. We find that $w_0(t)$ develops a sawtooth like profile [Fig. 3(b)] characteristic of avalanches and previously also observed in sheared foams and dense suspensions [12,36].

Next, we measure the sizes of the subsequently generated clusters in the dripping and irregular dripping modes [Fig. 3(c)]. Whereas in the former case the clusters are relatively monodisperse (yet much more polydisperse than in dripping of simple viscous fluids), in the latter case we observe recurring peaks in the cluster size corresponding to extremely large clusters. More quantitatively, in the dripping mode the number of grains N in a cluster does not apparently deviate from the Gaussian distribution. The coefficient of variation $CV_N = 19.5\%$ [see Fig. 3(d)] is significantly larger than in the case with the granular
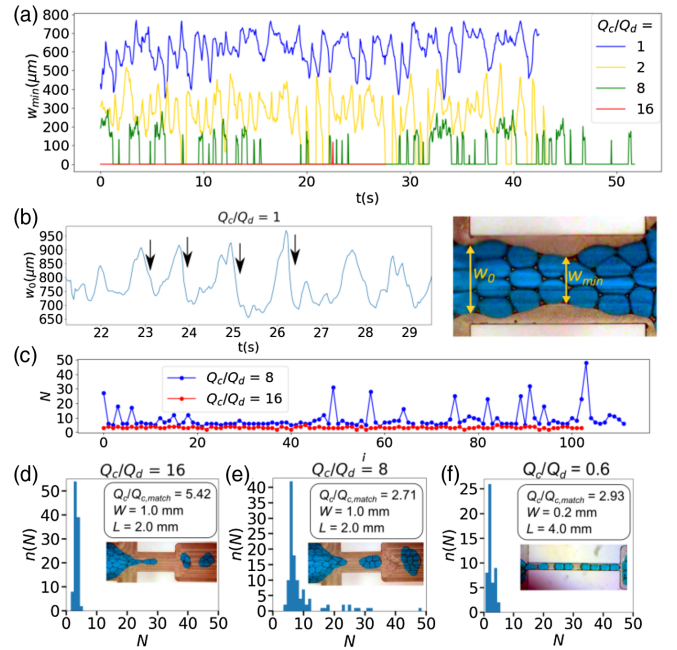

FIG. 3. (a) Fluctuations of the minimum jet width $w_{\min}(t)$ (b) Fluctuations of jet width $w_0(t)$ at the entrance to the constriction. The avalanching events are marked with arrows. (c) Number of grains N in clusters generated in the dripping and irregular dripping regimes ($Q_c/Q_d = 16$ and 8) vs the index of cluster i in order of generation, and (d)–(e) the corresponding histograms $n(N)$. The histogram in (f) shows analogous data for a system with a much thinner and longer orifice, yet with $Q_c/Q_{c,\text{match}}$ very close to the case in (e) (see main text and Supplemental Material [32] for further discussion).

emulsion replaced by the pure oil phase ($CV_{A_\parallel} = 2.2\%$), yet still moderate. In contrast, in the irregular dripping mode the distribution of cluster sizes N features a long right tail for large N [see Fig. 3(e)], with $CV_N = 74.3\%$ and a very large skewness, as documented by a Pearson's moment coefficient of skewness (see Supplemental Material [32] for a formal definition) $S_N = 3.1$.

We associate the formation of the extremely large clusters in the irregular dripping regime with the emergence of single-file chains of grains within the narrowing, which, once formed, exhibit remarkable stability. In principle, such chains remain stable once the local velocity of the continuous phase around the chain U_c matches the velocity of the grains inside the chain $U_{d,\text{chain}}$, which in turn is set by the rate of feeding of the grains into the orifice (note that this condition also determines the boundary between the dripping and jetting modes). Considering that $U_c = Q_c/[H \times (W - W_{\text{chain}})]$ and $U_{d,\text{chain}} = Q_d/(H \times W_{\text{chain}})$, where W_{chain} is the width of the chain, the requirement $U_c = U_{d,\text{chain}}$ leads to the following condition on the matching flow rate of the continuous fluid $Q_{c,\text{match}}$:

$$Q_{c,\text{match}}/Q_d = W/W_{\text{chain}} - 1. \tag{1}$$

We note that this requirement resembles the condition for continuity of soft polymer fibers stretched by an accelerating co-flow, studied by Mercader *et al.* [37]. In fact, our granular chains resemble semisolid fibers rather than viscous jets as demonstrated by (i) the lack of the Rayleigh-Plateau instability (typical of viscous jets) [25] and (ii) longitudinal stretching and/or compression of the chain as visualized by droplet deformations within the constriction, see Fig. 4(a). We associate such elastic solidlike behavior with a combination of the capillary arrest and deformability of the droplets within the chain.

From the experimentally measured average width of chain $W_{\text{chain}} = 0.68D_{\parallel} = 0.253W$ we obtain $Q_{c,\text{match}}/Q_d = 2.95$. This is close to the value $Q_c/Q_d = 2$ corresponding to the oscillating jetting regime; however, we actually observe single-file chains more often when $Q_c/Q_d = 8$, in the irregular dripping mode. We suspect that the relative scarcity of single-file chains for $Q_c/Q_d = 2$ results from spontaneous "folding" of single-file chains into wider jets
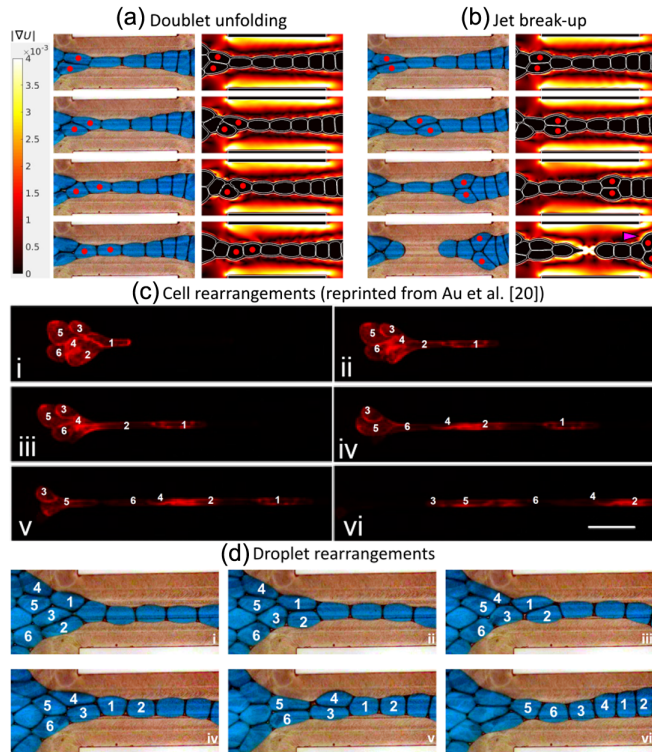

FIG. 4. (a)–(b) Numerical (at $Q_c/Q_d = 3.5$) and experimental (at $Q_c/Q_d = 8$) snapshots (see SM14 and SM15 [32], respectively, for the full movies) visualizing (a) doublet unfolding upon entry into the constriction and (b) a failure of unfolding, leading to an increased velocity gradient ∇U around the doublet (pink marker in the simulation panel) and breakup of the jet. (c) The order of entry of circulating tumor cells (CTCs) forming a cluster in a narrowing channel under co-flow (figure adapted with permission from Au *et al.* [20]; copyright National Academy of Sciences 2016) and (d) the order of entry of droplets into the constriction in our experiment, at $Q_c/Q_d = 8$ (see SM16 [32] for the full movie).

in the immediate vicinity of the theoretical matching velocity $U_{d,\text{chain}}$ (see SM2, seconds 1.83–2.58, 5.20–5.88, 24.01–24.76 [32]). At the same time, due to the finite length of the orifice L, chains are able to survive extensional stresses at $Q_c \gtrsim Q_{c,\text{match}}$, which may explain their abundance at $Q_c/Q_d = 8$.

We note that even at matched velocities the chains can break due to irregularity of the grain feeding into the orifice associated with stochasticity of grain rearrangements upon approaching the constriction. When a pair of grains enter the narrowing simultaneously they may rearrange, or "unfold," into a chain or not- in the latter case entering as a two-grain cluster or a "fold" (see Fig. 4). When the fold enters the orifice the continuous phase needs to locally accelerate and pass around it to conserve flux. The increased viscous forces acting at the fold result in chain stretching via longitudinal grain deformation which may eventually cause chain breakup.

Our LB simulations allow us to extract precise information about the velocity gradients within the system and verify this scenario. Indeed, we find progressively increasing velocity gradients around the doublet [see the purple marker in the last snapshot of Fig. 4(b)]. We propose that a similar mechanism (i.e., the acceleration of the continuous phase around wider parts of the jet) might also lead to the enhancement of fluctuations of jet width in the jetting and the oscillating jetting modes.

Next, we also perform a series of experiments with a smaller width of the orifice ($W \lesssim D_{\parallel}$), for which a simultaneous entry of two grains into the narrowing is hindered (see Supplemental Material [32] for details). In this case, the complex dynamical picture is lost and we only observe a transition between single-file jetting and dripping. To provide an example, we quantify the cluster size distribution in this geometry in Fig. 3(f) when $Q_c/Q_{c,\text{match}}$ (which serves as a measure of proximity to the jetting-dripping transition) is almost identical as in the long-tailed irregular dripping mode [Fig. 3(e)]. We still observe strong polydispersity ($\text{CV}_N = 44\%$), however, no long tails ($S_N = 0.73$). This further confirms the impact of individual grain rearrangements and, more specifically, the manner in which the grains enter the constriction, on the fate of the entire system, including the large-scale stochastic behavior.

Finally, we provide an example of how granular rearrangements observed in our flow-focusing setup could serve as a "benchmark" for more complex soft granular flows including confined biological flows. In fact, sequences of cell rearrangements have been previously studied in circulating tumor cell clusters transiting a narrowing channel [20]. Upon approaching a constriction the clusters were often able to unfold into a single-file chain without breakup. In some cases, the order in which the cells approached the narrowing seemed to determine their order of entry, but in some other cases the order was strongly disturbed by cell rearrangements [see Fig. 4(c)]. This is

interpreted in Ref. [20] as the effect of heterogeneity of cell-cell interactions and polydispersity of cells. However, our experiments demonstrate that even in a homogeneous, monodisperse *passive* granular system the order of entry is not strictly determined by the order of approach but rather depends on stochastic rearrangements upon entry [see Fig. 4(d)]. Accordingly, we argue that the phenomena reported by Au *et al.* [20] may result from the immanent irregularity of flow patterns associated with many-body interactions and general stochastic dynamics of soft granular media, and not only from heterogeneity of the grains.

In summary, we develop a model platform to study the behavior of soft granular media subjected to external flows and demonstrate rich phenomenology including stochastic granular jettinglike and drippinglike modes with no counterpart in simple fluids.

We note that series of two (or more) microfluidic junctions have been previously used to produce double-emulsion core-shell droplets with multiple cores [38–44]. A couple of recent works considered cores-in-shell volume fractions high enough ($> 80\%$) for the double-emulsion drops to be considered soft granular clusters [17,39,45,46]. However, those previous works exploited generation of the clusters via one-by-one feeding of the cores into the shell without actually considering the flow of a soft-granular medium *per se*. In this Letter, we argue that the latter poses a completely different problem and involves phenomena not present in simple fluids.

Our findings open up several avenues for future work. First, the full dynamical phase diagram in the three-dimensional (Q_c, Q_d, ϕ)-space including possible hysteretic behavior at transitions between the modes—also depending on the viscosities and interfacial tensions–remains to be established. Second, the statistics of rearrangements between individual grains could be further investigated to shed light on the effective phases of matter (solidlike vs fluidlike) occurring in such a system. Finally, our platform could also be further developed to allow tracking of the internal relaxation dynamics of the generated granular clusters. This poses possible significance, e.g., to the recovery of tissues after mechanical injury or the dynamics of CTCs in capillaries during cancer metastasis.

---

[*]mbogdan@ichf.edu.pl
[†]jguzowski@ichf.edu.pl

[1] K. Guevorkian, M. J. Colbert, M. Durth, S. Dufour, and F. Brochard-Wyart, Aspiration of Biological Viscoelastic Drops, Phys. Rev. Lett. **104**, 218101 (2010).

[2] S. Douezan, K. Guevorkian, R. Naouar, S. Dufour, D. Cuvelier, and F. Brochard-Wyart, Spreading dynamics and wetting transition of cellular aggregates, Proc. Natl. Acad. Sci. U.S.A. **108**, 7315 (2011).

[3] M. L. Manning, R. A. Foty, M. S. Steinberg, and E.-M. Schoetz, Coaction of intercellular adhesion and cortical tension specifies tissue surface tension, Proc. Natl. Acad. Sci. U.S.A. **107**, 12517 (2010).

[4] S. Cohen-Addad, R. Höhler, and O. Pitois, Flow in foams and flowing foams, Annu. Rev. Fluid Mech. **45**, 241 (2013).

[5] S. Nezamabadi, T. H. Nguyen, J. Y. Delenne, and F. Radjai, Modeling soft granular materials, Granular Matter **19**, 8 (2017).

[6] A. A. J. Kabla, Collective cell migration: Leadership, invasion and segregation, J. R. Soc. Interface **9**, 3268 (2012).

[7] S. Pawlizak, A. W. Fritsch, S. Grosser, D. Ahrens, T. Thalheim, S. Riedel, T. R. Kiessling, L. Oswald, M. Zink, M. L. Manning, and J. A. Käs, Testing the differential adhesion hypothesis across the epithelial-mesenchymal transition, New J. Phys. **17**, 083049 (2015).

[8] Y. Gai, C. M. Leong, W. Cai, and S. K. Tang, Spatiotemporal periodicity of dislocation dynamics in a two-dimensional microfluidic crystal flowing in a tapered channel, Proc. Natl. Acad. Sci. U.S.A. **113**, 12082 (2016).

[9] Y. Gai, J. W. Khor, and S. K. Tang, Confinement and viscosity ratio effect on droplet break-up in a concentrated emulsion flowing through a narrow constriction, Lab Chip **16**, 3058 (2016).

[10] Y. Jiang, P. J. Swart, A. Saxena, M. Asipauskas, and J. A. Glazier, Hysteresis and avalanches in two-dimensional foam rheology simulations, Phys. Rev. E **59**, 5819 (1999).

[11] P. Marmottant and F. Graner, Plastic and viscous dissipations in foams: Cross-over from low to high shear rates, Soft Matter **9**, 9602 (2013).

[12] P. Kumar, E. Korkolis, R. Benzi, D. Denisov, A. Niemeijer, P. Schall, F. Toschi, and J. Trampert, On interevent time distributions of avalanche dynamics, Sci. Rep. **10**, 1 (2020).

[13] J. Goyon, A. Colin, G. Ovarlez, A. Ajdari, and L. Bocquet, Spatial cooperativity in soft glassy flows, Nature (London) **454**, 84 (2008).

[14] J. Goyon, A. Colin, and L. Bocquet, How does a soft glassy material flow: finite size effects, non local rheology, and flow cooperativity, Soft Matter **6**, 2668 (2010).

[15] M. Lulli, R. Benzi, and M. Sbragaglia, Metastability at the Yield-Stress Transition in Soft Glasses, Phys. Rev. X **8,** 021031 (2018).

[16] M. D. Uchic, D. M. Dimiduk, J. N. Florando, and W. D. Nix, Sample dimensions influence strength and crystal plasticity, Science **305,** 986 (2004).

[17] M. Constantini, J. Guzowski, P. J. Żuk, P. Mozetic, S. De Panfilis, J. Jaroszewicz, M. Heljak, M. Massimi, M. Pierron, M. Trombetta, M. Dentini, W. Święszkowski, A. Rainer, P. Garstecki, and A. Barbetta, Electric field assisted microfluidic platform for generation of tailorable porous microbeads as cell carriers for tissue engineering, Adv. Funct. Mater. **28,** 1 (2018).

[18] M. Constantini, J. Jaroszewicz, Ł. Kozoń, K. Szlązak, W. Święszkowski, P. Garstecki, C. Stubenrauch, A. Barbetta, and J. Guzowski, 3D printing of functionally graded porous materials using on-demand reconfigurable microfluidics, Angew. Chem. **131,** 7702 (2019).

[19] C. B. Highley, K. H. Song, A. C. Daly, and J. A. Burdick, Jammed microgel inks for 3D printing applications, Adv. Sci. **6,** 1801076 (2019).

[20] S. H. Au, B. D. Storey, J. C. Moore, Q. Tang, Y. L. Chen, S. Javaid, A. F. Sarioglu, R. Sullivan, M. W. Madden, R. O'Keefe, D. A. Haber, S. Maheswaran, D. M. Langenau, S. L. Stott, and M. Toner, Clusters of circulating tumor cells traverse capillary-sized vessels, Proc. Natl. Acad. Sci. U.S.A. **113,** 4947 (2016).

[21] J. P. Raven and P. Marmottant, Microfluidic Crystals: Dynamic Interplay between Rearrangement Waves and Flow, Phys. Rev. Lett. **102,** 084501 (2009).

[22] P. Garstecki and G. M. Whitesides, Flowing Crystals: Nonequilibrium Structure of Foam, Phys. Rev. Lett. **97,** 024503 (2006).

[23] S. L. Anna, N. Bontoux, and H. A. Stone, Formation of dispersions using "flow focusing" in microchannels, Appl. Phys. Lett. **82,** 364 (2003).

[24] C. N. Baroud, F. Gallaire, and R. Dangla, Dynamics of microfluidic droplets, Lab Chip **10,** 2032 (2010).

[25] A. S. Utada, A. Fernandez-Nieves, H. A. Stone, and D. A. Weitz, Dripping to Jetting Transitions in Coflowing Liquid Streams, Phys. Rev. Lett. **99,** 094502 (2007).

[26] T. Cubaud and T. G. Mason, Capillary threads and viscous droplets in square microchannels, Phys. Fluids **20,** 053302 (2008).

[27] N. M. Kovalchuk, M. Sagisaka, K. Steponavicius, D. Vigolo, and M. J. Simmons, Drop formation in microfluidic cross-junction: Jetting to dripping to jetting transition, Microfluid. Nanofluid. **23,** 103 (2019).

[28] A. Montessori, M. Lauricella, N. Tirelli, and S. Succi, Mesoscale modelling of near-contact interactions for complex flowing interfaces, J. Fluid Mech. **872,** 327 (2019).

[29] A. Montessori, M. Lauricella, A. Tiribocchi, and S. Succi, Modeling pattern formation in soft flowing crystals, Phys. Rev. Fluids **4,** 072201 (2019).

[30] S. Succi, *The Lattice Boltzmann Equation: For Complex States of Flowing Matter* (Oxford University Press, 2018).

[31] C. Holtze, A. C. Rowat, J. J. Agresti, J. B. Hutchison, F. E. Angilè, C. H. Schmitz, S. Köster, H. Duan, K. J. Humphry, R. A. Scanga, J. S. Johnson, D. Pisignano, and D. A. Weitz, Biocompatible surfactants for water-in-fluorocarbon emulsions, Lab Chip **8,** 1632 (2008).

[32] See Supplemental Material at http://link.aps.org/supplemental/10.1103/PhysRevLett.128.128001 for additional information, data and video documentation.

[33] A. Montessori, A. Tiribocchi, M. Lauricella, F. Bonaccorso, and S. Succi, Mesoscale modelling of droplets' self-assembly in microfluidic channels, Soft Matter **17,** 2374 (2021).

[34] At such Q_d the emulsion was possibly most stable.

[35] P. Garstecki, M. J. Fuerstman, and G. M. Whitesides, Nonlinear Dynamics of a Flow-Focusing Bubble Generator: An Inverted Dripping Faucet, Phys. Rev. Lett. **94,** 234502 (2005).

[36] D. J. Durian, Foam Mechanics at the Bubble Scale, Phys. Rev. Lett. **75,** 4780 (1995).

[37] C. Mercader, A. Lucas, A. Derré, C. Zakri, S. Moisan, M. Maugey, and P. Poulin, Kinetics of fiber solidification, Proc. Natl. Acad. Sci. U.S.A. **107,** 18331 (2010).

[38] S. Okushima, T. Nisisako, T. Torii, and T. Higuchi, Controlled production of monodisperse double emulsions by two-step droplet breakup in microfluidic devices, Langmuir **20,** 9905 (2004).

[39] D. Lee and D. A. Weitz, Nonspherical colloidosomes with multiple compartments from double emulsions, Small **5,** 1932 (2009).

[40] J. Wan, A. Bick, M. Sullivan, and H. A. Stone, Controllable microfluidic production of microbubbles in water-in-oil emulsions and the formation of porous microparticles, Adv. Mater. **20,** 3314 (2008).

[41] A. R. Abate and D. A. Weitz, High-order multiple emulsions formed in poly(dimethylsiloxane) microfluidics, Small **5,** 2030 (2009).

[42] L. L. Adams, T. E. Kodger, S. H. Kim, H. C. Shum, T. Franke, and D. A. Weitz, Single step emulsification for the generation of multi-component double emulsions, Soft Matter **8,** 10719 (2012).

[43] A. S. Utada, E. Lorenceau, D. R. Link, P. D. Kaplan, H. A. Stone, and D. A. Weitz, Monodisperse double emulsions generated from a microcapillary device, Science **308,** 537 (2005).

[44] G. T. Vladisavljević, R. Al Nuumani, and S. A. Nabavi, Microfluidic production of multiple emulsions, Micromachines **8,** 75 (2017).

[45] J. Guzowski and P. Garstecki, Droplet Clusters: Exploring the Phase Space of Soft Mesoscale Atoms, Phys. Rev. Lett. **114,** 188302 (2015).

[46] S. H. Kim, H. Hwang, C. H. Lim, J. W. Shim, and S. M. Yang, Packing of emulsion droplets: Structural and functional motifs for multi-cored microcapsules, Adv. Funct. Mater. **21,** 1608 (2011).